Electronic Supplementary Material (ESI) for Physical Chemistry Chemical Physics.

Shape Selectivity of Corannulene dimer based on Concave−Convex and Convex−Convex Shape Complementary as Hosts for C_{60} and C_{70}

Li Wang*[a], Yan-Li Liu[a], Sheng-Hui Chen[a], De He[a], Quan-Jiang Li[a], Mei-Shan Wang*[a]

[a]*School of Physics and Optoelectronics Engineering, Ludong University, Yantai, 264025, Shandong, China.*

E-mail: wangl@ldu.edu.cn (L. Wang); mswang1971@163.com (M. S. Wang)

†Electronic supplementary information (ESI) available: The components of the total polarizability α (a.u.) and the second hyperpolarizabilities γ (a.u.) for the studied complexes.

Table S1. The stabilization energies (a.u.) and the energy differences (Egap) between the HOMO and the LUMO (E_{gap}, eV) of complexes.

Complex	Energy		E_{gap}	
	a	*b*	*a*	*b*
1	-3823.021883	-3823.020318	2.68	2.67
2	-3823.003116	-3823.002932	2.67	2.66
3	-3822.986294	-3822.986163	2.64	2.63
4	-4204.206946	-4204.185339	2.71	2.66
5	-4204.189336	-4204.188280	2.69	2.66
6	-4204.171613	-4204.171601	2.67	2.63

In the process of structural optimization, there are four criteria for structural convergence including the Maximum Force (MS) value less than 0.00045, the Root-Mean-Square Force (RF) less than 0.00030, the Maximum Displacement (MD) value less than 0.00180 and the RMS Displacement (RD) value less than 0.00120. The force causing molecular structure deformation becomes smaller and smaller, that is, the structure gradually tends to be stable during the optimization process. Similarly, displacement is also the parameter of deformation. When both of them meet the standard of convergence, the molecule can be considered stable. From the Table S2, all the optimized structures satisfy four limits of convergence, so the structures are stable.

Table S2. The settings and tolerance factors on the Energy (E) and forces including Maximum Force (MS), RMS Force (RF), Maximum Displacement (MD) and RMS Displacement (RD) used for geometric relaxation.

	MF		RF		MD		RD		E
	Value	Threshold	Value	Threshold	Value	Threshold	Value	Threshold	
1	0.000014	0.00045	0.000002	0.0003	0.000627	0.0018	0.000121	0.0012	-2.689×10^{-8}
2	0.000025	0.00045	0.000003	0.0003	0.000967	0.0018	0.000176	0.0012	-2.344×10^{-8}
3	0.00003	0.00045	0.000005	0.0003	0.001182	0.0018	0.000248	0.0012	-2.010×10^{-7}
4	0.000013	0.00045	0.000003	0.0003	0.000268	0.0018	0.000055	0.0012	-1.080×10^{-7}
5	0.000011	0.00045	0.000002	0.0003	0.000965	0.0018	0.000161	0.0012	-3.692×10^{-8}
6	0.000021	0.00045	0.000003	0.0003	0.000260	0.0018	0.000063	0.0012	-3.425×10^{-8}

In the structural optimization, B3LYP-D3 is the most cost-effective method for large systems with weak interaction. This is because that DFT-D3 is more rigorous than DFT-D2 which is tagged at the time of the functional B97D definition. DFT-D3 has better overall precision and provides parameters for almost all mainstream functionals, and hardly adds any computing time. It is also easy to implement. Almost all mainstream quantifiers now support DFT-D3. In the hybrid functional, the precision of B3LYP-D3 is among the highest, which can be seen in the Table 20 of the supplementary materials of Ref Phys. Chem. Chem. Phys., 19, 32184 (2017).

Table S3. The geometric structure parameters of complex **1** obtained by B3LYP-D3/6-31G(d), B3LYP-D3/6-31+G(d) and B97D/6-31+G(d) levels.

Parameter	B3LYP-D3/6-31G(d)	B3LYP-D3/6-31+G(d)	B97D/6-31+G(d)
Layer distance (Å)	3.47	3.49	3.42
HF energy (a.u.)	-3823.0	-3823.1	-3819.7
E_{gap} (eV)	2.68	2.62	1.54

Table S4. The components of the total polarizability α (a.u.) for the studied complexes.

Complex	Method	α_{xx}	α_{yy}	α_{zz}
1	CAM-B3LYP	910.6	910.6	963.9
	BHandHLYP	909.4	909.4	965.6
2	CAM-B3LYP	939.3	939.1	999.3
	BHandHLYP	937.8	937.6	1003.8
3	CAM-B3LYP	968.7	968.7	1027.8
	BHandHLYP	966.9	966.9	1034.6
4	CAM-B3LYP	1005.6	1005.6	1159.0
	BHandHLYP	1005.6	1005.7	1164.5
5	CAM-B3LYP	1035.9	1035.9	1197.6
	BHandHLYP	1035.7	1035.8	1206.8
6	CAM-B3LYP	1066.3	1066.3	1234.2
	BHandHLYP	1065.9	1065.9	1246.9

Table S5. The components of the second hyperpolarizabilities γ (a.u.) for the studied complexes.

Complex	Method	γ_{xxxx}	γ_{yyyy}	γ_{zzzz}	γ_{xxyy}	γ_{xxzz}	γ_{yyzz}
1	CAM-B3LYP	193153.0	193187.0	553752.0	64384.1	72486.4	72518.6
	BHandHLYP	195924.0	195967.0	574061.0	65302.7	74136.0	74162.6
2	CAM-B3LYP	195624.0	195600.0	1705390.0	65186.2	82431.2	82496.9
	BHandHLYP	197384.0	197360.0	1924070.0	65764.6	86411.0	86482.6
3	CAM-B3LYP	200012.0	200045.0	2726590.0	66673.8	90445.8	90457.8
	BHandHLYP	200748.0	200780.0	3117210.0	66915.3	96243.1	96255.9
4	CAM-B3LYP	203996.0	204063.0	843627.0	67987.6	120872.0	120953.0
	BHandHLYP	204943.0	205014.0	900861.0	68303.1	124361.0	124441.0
5	CAM-B3LYP	207857.0	207922.0	2573110.0	69290.6	139444.0	139506.0
	BHandHLYP	207703.0	207770.0	2949100.0	69236.1	146381.0	146443.0
6	CAM-B3LYP	211244.0	211315.0	4185480.0	70425.3	155869.0	155924.0
	BHandHLYP	209865.0	209936.0	4860070.0	69962.7	165668.0	165726.0

Table S6. The components of the total polarizability α (a.u.) for the complex **1** computed at BHandHLYP/6-31+G(d) level under the external electric fields of 10×10^{-4}, 20×10^{-4}, 30×10^{-4}, 40×10^{-4}, 50×10^{-4} a.u...

Field (10^{-4} a.u.)	α_{xx}	α_{yy}	α_{zz}	α_{tot}
0	909.4	909.4	965.6	928.1
10	909.5	909.5	965.7	928.2
20	908.5	908.1	967.9	928.1
30	909.4	909.4	966.3	928.4
40	909.3	909.3	966.8	928.5
50	909.2	909.2	967.4	928.6

Table S7. The components of the second hyperpolarizabilities γ (a.u.) for the complex **1** computed at BHandHLYP/6-31+G(d) level under the external electric fields of 10×10^{-4}, 20×10^{-4}, 30×10^{-4}, 40×10^{-4}, 50×10^{-4} a.u...

Field (10^{-4} a.u.)	γ_{xxxx}	γ_{yyyy}	γ_{zzzz}	γ_{xxyy}	γ_{xxzz}	γ_{yyzz}	γ_{tot}
0	195924.0	195967.0	574061.0	65302.7	74136.0	74162.6	278630.9
10	196194.0	196224.0	579876.0	65381.5	74318.5	74358.2	280082.1
20	196638.0	195639.0	607161.0	65031.3	74475.2	74235.9	285384.6
30	196175.0	196202.0	585800.0	65372.4	74354.6	74397.7	281285.3
40	196141.0	196166.0	590149.0	65359.8	74392.2	74438.1	282167.2
50	196096.0	196118.0	595560.0	65343.1	74444.4	74497.1	283268.6

Among them, the position *c* is unreasonable to complex another $C_{20}H_{10}$ ring, which is due to that the atoms of two $C_{20}H_{10}$ ring are too close, leading to that the geometric optimizations of complexes **1*c*** ~ **6*c*** cannot be performed normally. Theoretically, position *a* is the most stable structure because the repulsion is weakest. To test our guess, complexes **1*a*** (**1*b***) ~ **6*a*** (**6*b***) were optimized by B3LYP-D3/6-31G(d) level. The results show that the structures **1*b*** ~ **6*b*** have certain degree of structural deformations and the calculation results of single point energy show that structures **1*b*** ~ **6*b*** possess higher stabilization energies with respect to that of **1*a*** ~ **6*a*** (Table S1). Therefore, **1*a*** ~ **6*a*** are most stable structures. In the main text, the complexes **1*a*** ~ **6*a*** were named as **1** ~ **6**.

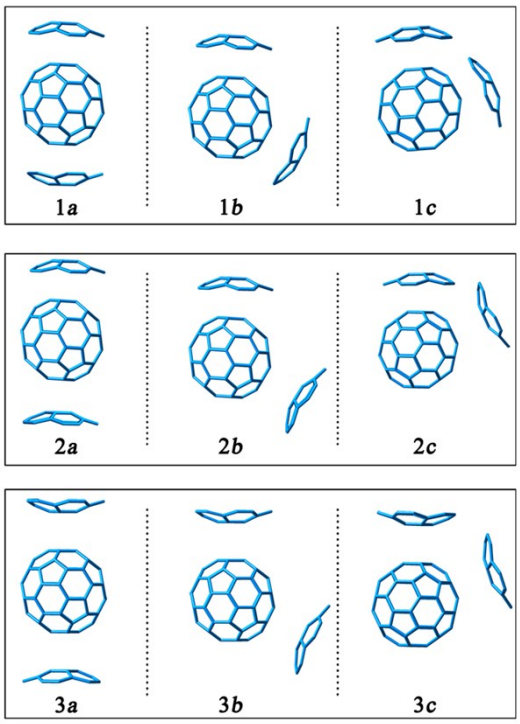

Figure S1. Possible structures of complexes $2C_{20}H_{10}/C_{60}$.

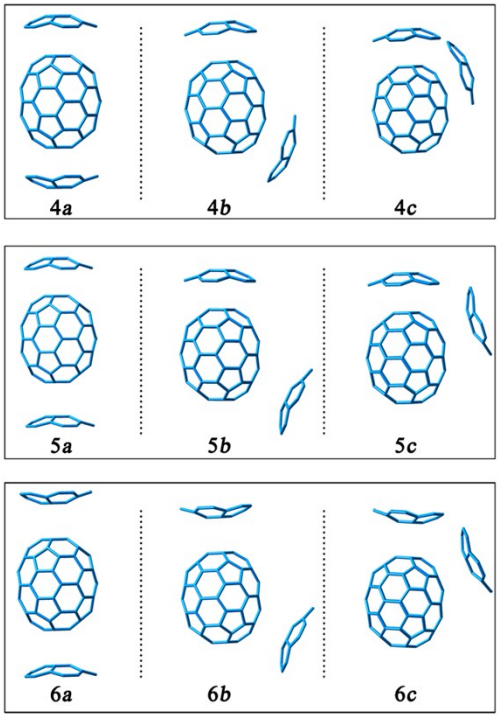

Figure S2. Possible structures of complexes $2C_{20}H_{10}/C_{70}$.

For the sake of reliable simulation results, the comparison between the theoretical analog spectra in o-dichlorobenzene solvent and the experimental results of C_{60}:$C_{28}H_{14}$ and C_{70}:2$C_{28}H_{14}$ in o-dichlorobenzene solvent[32] have been executed (Figure S). The simulated spectra of C_{60}:$C_{28}H_{14}$ by TD-B3LYP functional have only one maximum absorption peak at 360 nm, which is different from the experimental spectrum. While, the simulated spectra of C_{60}:$C_{28}H_{14}$ by TD-CAM-B3LYP have two absorption peaks at 315 nm and 425 nm, which are relatively close to the experimental spectra at 336 nm and 410 nm with respect that of B3LYP. Similarly, compared with the the simulated spectra by B3LYP of C_{70}:2$C_{28}H_{14}$, the spectra obtained by CAM-B3LYP at 363 nm and 471 nm was closer to its two absorption peaks of experimental spectra at 383 nm and 474 nm. It reveals that the B3LYP functional underestimates the excitation energy of the maximum absorption peak

largely, while the simulated spectra by means of the CAM-B3LYP functional were close to the experimental results. Therefore, for the studied complexes, the result of TD-CAM-B3LYP is chosen to simulate absorption spectra of the studied complexes.

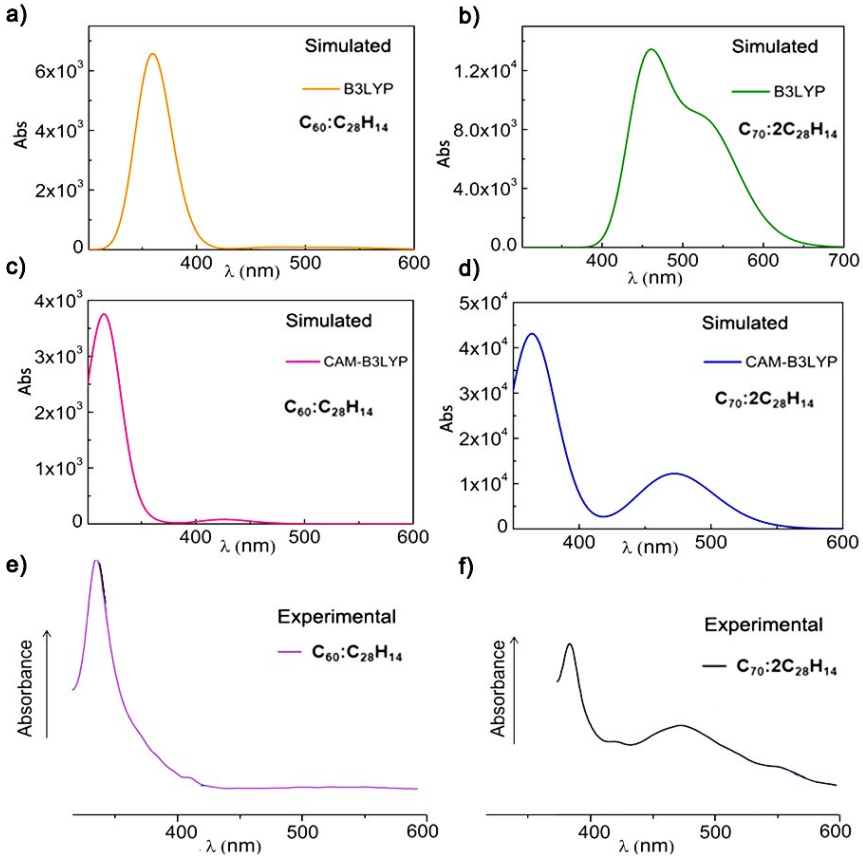

Figure S3. Simulated UV−Vis spectra of C_{60}:$C_{28}H_{14}$ and C_{70}:$2C_{28}H_{14}$ in o-dichlorobenzene solvent at TD-B3LYP/6-31+G(d) and TD-CAM-B3LYP/6-31+G(d) level of theory and their experimental spectra[32].